



Constraining the age of Quaternary megafloods in the Altai Mountains (Russia) using luminescence

M.I. Svistunov^{a,*,1}, R.N. Kurbanov^b, A.S. Murray^c, N.A. Taratunina^d, D.V. Semikolennykh^e, A.L. Entin^f, Ye.V. Deev^{g,h}, I.D. Zolnikov^g, A.V. Paninⁱ

^a *Otkrytoye Shosse, 2/10, 49, 107143 Moscow, Russia*

^b *Leninskie Gory, GSP-1, 119991 Moscow, Russia*

^c *Department of Geoscience, Aarhus University, Høegh-Guldbergs Gade 2, DK-8000c Aarhus, Denmark*

^d *Proizvodstvennaya St., 8/1, 119619, Moscow, Russia*

^e *Dovzhenko St. 12/2, 119285 Moscow, Russia*

^f *Vorobiovy Gory 1, 119234 Moscow, Russia*

^g *Akademika Koptuyuga Ave. 3, 630090 Novosibirsk, Russia*

^h *Lenin Ave. 36, 634050 Tomsk, Russia*

ⁱ *Staromonetny Pereulok 29, 119017 Moscow, Russia*

ARTICLE INFO

Keywords:

Megaflod deposits
Catastrophic events
Russian Altai
Loess
Luminescence dating

ABSTRACT

Some of the largest catastrophic outbursts of periglacial lakes known in the geological history of the Earth have been identified in the Altai Mountains. Traces of these events are recorded in the form of large terraces, predominantly composed of gravel material with numerous horizons of large boulders and blocks. Determining the age of these large-scale events is difficult due to the lack of suitable material (e.g. organics, well-bleached sand) and the specific genesis of these sediments. The results of cosmogenic radionuclide dating suggest a post-LGM age both for the source of the flood water and for different elements of the catafluvial terraces in the Chuya and Katun river valleys. Nevertheless, the age(s) of catastrophic breakthrough remains controversial. On the basis of a few IRSL ages, and geological and other evidence, some view the event as occurring around MIS 5. In this study, we investigate loess-like loams overlying the catafluvial sediments on the surface of the highest level terrace, ~200 m above present river level. A total of 24 samples for luminescence dating were obtained, for which the OSL, IR₅₀, and pIRIR_{50,290} signals were measured to control the degree of signal zeroing and the dating reliability. The age of the loess in all three pits was from 0.5 ka at the top to 23 ka at the base of the loess strata. From a sand layer in the top of the catafluvial deposits, two ages of ~85–90 ka were obtained from feldspar pIRIR_{50,290}. These results provide a minimum pre-LGM age for the geomorphological surface of a major catafluvial terrace in the Altai Mountains.

1. Introduction

The Russian Altai is a classical region in Russian glacial geomorphology, and the resulting large data set makes the Altai a very suitable test area for understanding the glacial superflooding that has left abundant morphological evidence throughout several river valleys; this event (or events) is ranked as one of the largest catastrophic floods in the geological history of the Earth (Baker et al., 1993; Rudoj, 1995; Herget, 2005; Baker, 2013). Discussion of the descriptive parameters and timing of these floods is directly related to the glacial history, and

has been going on for more than three decades. It is also recognised that seismic events may have triggered dam failure, by destabilising moraine and ice dams. Only reliable direct geochronological data can further these debates. A new major Russian project (RSF 19-17-00179) is currently undertaking a comprehensive study of the history of catastrophic events in the Russian Altai; primary glacial formations and related structures, limno-glacial, fluvio-glacial deposits, and seismic phenomena are all being described and, where possible, dated. This study is a contribution to this research.

The discovery of sediments and landforms associated with glacial

* Corresponding author.

E-mail address: svistunov.mi@yandex.ru (M.I. Svistunov).

¹ Please see acknowledgements.

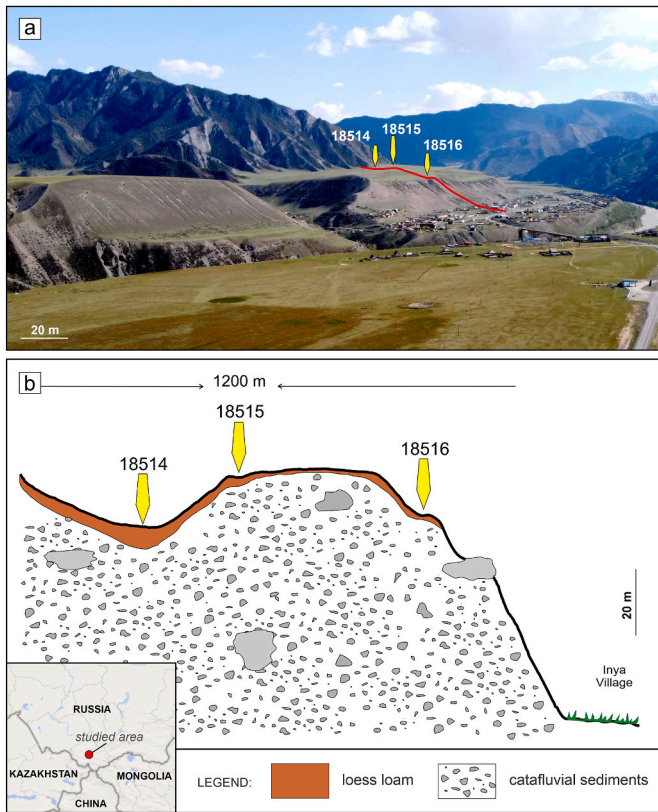


Fig. 1. Site location, general view of the Inya terrace and location of the three sampling pits.

superflooding in the Altai Mountains was first published Rudoy and Baker (1993), Butvilovskij (1993) and Rudoy (2002). Parnachev (1999) undertook facies-genetic analysis of superflood deposits and a comparison with similar genetic types; he identified and described a typical flood cyclite in the Yaloman-Katun zone of the Gorny Altai. Carling

(2013) synthesized the mechanisms of megaflood sedimentation on Earth with special emphasize to the Altai catafluvial deposits. Since the early 1990s, the scabland (a territory that has experienced the effects of catastrophic water flows in the past) of Gorny Altai has been actively visited by several international expeditions (Carling et al., 2002, 2016; Herget, 2005; Reuther et al., 2006; Lehmkuhl et al., 2006 and others), and two major international meetings have been held to discuss the area (Buylaert et al., 2015; Krivonogov et al., 2017). Estimates for different stages of the flood, and different sections of the Katun and Chuya rivers downstream from the collapsed glacial dam suggest water discharges

Table 1
Section descriptions.

Layer	Depth, m	Description
18514 pit		
1	0,0–0,40	Brown non-layered clayey silt with occasional inclusions of fine gravel, some permafrost deformation.
2	0,40–0,75	Light brown silt with occasional inclusions of fine gravel and plant roots.
3	0,75–0,90	Gray sandy silt with inclusions of gravel and sometimes fine gravel, penetrated by vertical cracks up to 1.0–1.5 cm in diameter, filled with brown silt of layer 2 (traces of roots).
4	0,90–1,10	Gray fine-grained sand, non-layered
5	1,10–1,90	Light gray horizontally layered fine-grained sand with interlayers (1.5–2.0 cm thick) of coarse-medium-grained darker sand with pebble inclusions at a depth of 1.70 m
6	1,90–2,10	Fine loose gravel with sand matrix. Probably the alluvium of the hollow is the washed-out alluvium of the terrace
18515 pit		
1	0,0–0,35	Light brown sandy loam with the inclusion of fine grus, the border with the underlying layer is clear
2	0,35–0,60	Brown sandy and silty loam
3	0,60–1,05	Light beige unstratified silt. There is a hole filled with layer 1 material in the right corner of cross-section
4	1,05–1,15	Light beige silt with small gravel
18516 pit		
1	0,0–0,35	Brown sandy loam with the inclusion of fine grus, the border with the underlying layer is clear
2	0,35–1,05	Light brown grayish silty loam with the inclusion of grus of different sizes
3	1,05–1,15	Fine gravel with loamy matrix

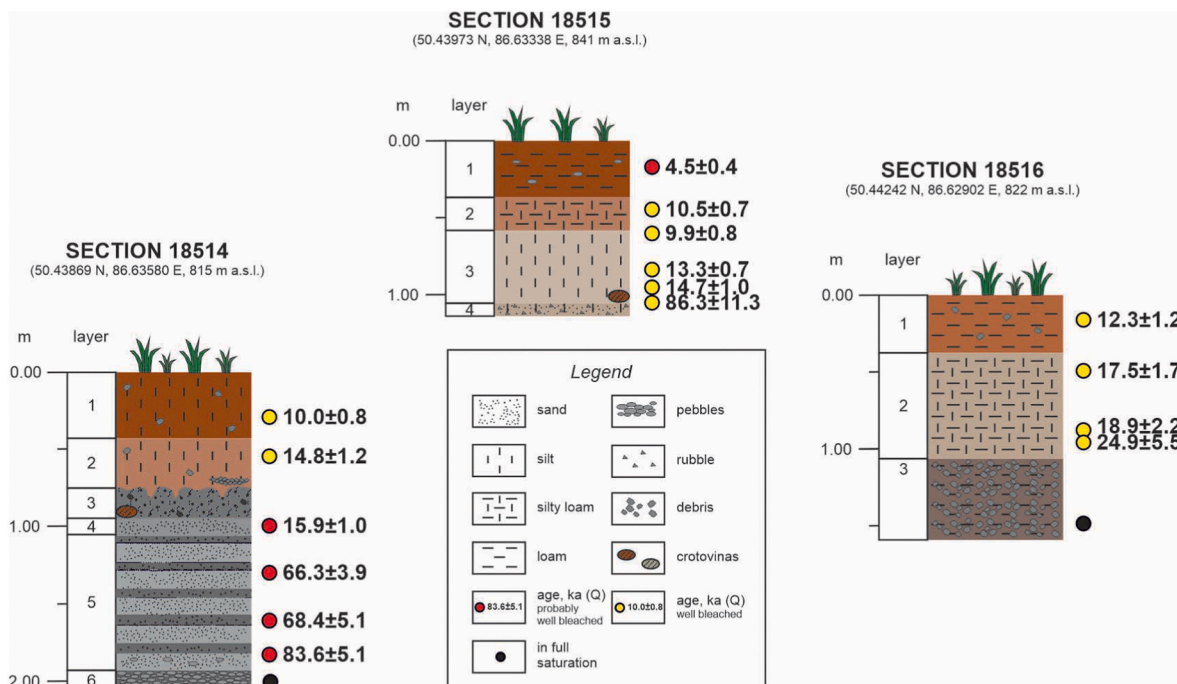


Fig. 2. Sections of the 3 pits dug on top of the Inya terrace. OSL ages are given in ka, quartz as filled red circles, feldspar pIRIR_{50,290} as filled yellow circle.

Table 2
Radionuclide concentrations, dry beta and gamma dose rates.

Lab N ^o	Depth, cm	²³⁸ U, Bq/kg	²²⁶ Ra, Bq/kg	²³² Th, Bq/kg	⁴ K, Bq/kg	Dry beta dose rate, Gy/ka	Dry gamma dose rate, Gy/ka
208871	20	42.0 ± 9.2	35.9 ± 0.8	41.1 ± 0.8	613 ± 13	2.18 ± 0.04	1.22 ± 0.03
208872	50	15.3 ± 9.8	33.5 ± 1.0	36.4 ± 0.9	526 ± 19	1.91 ± 0.05	1.08 ± 0.03
208873	80	32.3 ± 6.6	35.4 ± 0.6	38.4 ± 0.6	547 ± 13	1.99 ± 0.04	1.13 ± 0.03
208874	95	38.3 ± 10.0	40.4 ± 1.0	42.0 ± 0.9	557 ± 19	2.09 ± 0.06	1.22 ± 0.04
208875	150	30.9 ± 13.2	31.1 ± 1.1	37.2 ± 1.1	501 ± 17	1.83 ± 0.05	1.05 ± 0.03
208876	200	16.6 ± 3.8	18.8 ± 0.3	16.2 ± 0.3	367 ± 6	1.22 ± 0.02	0.61 ± 0.02
208877	180	15.6 ± 7.0	22.0 ± 0.6	16.0 ± 0.4	445 ± 11	1.45 ± 0.03	0.69 ± 0.02
208878	160	16.1 ± 9.0	22.7 ± 0.8	15.4 ± 0.6	460 ± 15	1.49 ± 0.04	0.70 ± 0.02
208879	130	23.2 ± 4.3	21.2 ± 0.4	16.3 ± 0.4	428 ± 9	1.40 ± 0.03	0.68 ± 0.02
208880	100	22.9 ± 5.4	21.5 ± 0.4	15.0 ± 0.5	459 ± 8	1.47 ± 0.03	0.69 ± 0.02
208881	55	30.5 ± 7.6	31.1 ± 0.7	28.9 ± 0.5	493 ± 12	1.75 ± 0.04	0.95 ± 0.03
208882	30	27.5 ± 7.6	30.3 ± 0.7	28.0 ± 0.5	469 ± 12	1.68 ± 0.04	0.91 ± 0.03
208883	105	25.7 ± 4.2	18.7 ± 0.3	14.5 ± 0.4	330 ± 6	1.12 ± 0.02	0.56 ± 0.02
208884	95	32.4 ± 5.5	31.4 ± 0.4	30.9 ± 0.5	500 ± 8	1.78 ± 0.03	0.98 ± 0.03
208885	80	27.3 ± 6.0	32.3 ± 0.5	34.9 ± 0.6	504 ± 8	1.83 ± 0.03	1.03 ± 0.03
208886	65	31.6 ± 6.5	36.9 ± 0.5	40.1 ± 0.6	556 ± 9	2.04 ± 0.03	1.17 ± 0.03
208887	45	28.2 ± 8.8	42.7 ± 0.8	46.0 ± 0.7	726 ± 16	2.57 ± 0.05	1.41 ± 0.04
208888	20	35.4 ± 9.6	47.1 ± 0.9	47.8 ± 0.7	736 ± 19	2.65 ± 0.06	1.47 ± 0.04

from 2×10^4 to 1.8×10^7 m³/s, water depths from 50 to 400 m, and flow velocities from 16 to 72 m/s (Baker et al., 1993; Rudoj, 2001; Herget 2005; Carling et al., 2010). The flood duration is thought to have been from one and a half days up to 2 weeks (Rudoj, 2001; Huang et al., 2014; Bohorquez et al., 2019), and it left behind a variety of geomorphological evidence, including giant terraces (Fig. 1) and vehicle-sized clasts deposited on the valley floor; all these are presumed to have been transported and deposited in only one or a very few individual floods.

There is currently no clear consensus on the age these super-flood events. Rudoj (2005) assumes that flood events occurred around 7, 12, 15, 17 and more than 22 ka ago. A series of Optically Stimulated Luminescence (OSL) ages suggest that the last super-floods took place much earlier, before the end of MIS-5 (Panin and Baryshnikov, 2015a,b;

Zolnikov et al., 2016, 2021). However another attempt to obtain a luminescence chronology for the Katun basin deposits showed that the sampled sediments were insufficiently bleached before deposition (Lehmkuhl et al., 2006).

In summary, the key difficulty in reconstructing the glacial and palaeo-flood history of the Altai is a lack of geochronology; this has arisen because of both complicated facies and lack of widespread organic matter for radiocarbon analysis, and, unexpectedly, sediments that are apparently older than the limits of the radiocarbon dating method. In this study, we contribute to addressing this problem by dating loess-like sediments on top of the largest and most elevated of the catafluvial terraces. The target material is known to be very suitable for luminescence dating and so these ages should provide a secure minimum age for the deposition of the terrace sediments. We use a comparison of both quartz and feldspar OSL signals to confirm the sufficiency of bleaching before final deposition, and compare these results with ages from sands incorporated into the top of the terraces themselves.

2. Study area, site description and sampling

The study site is located on the right side of the Katun river, where catafluvial terraces are most pronounced. Near the village of Inya, two catafluvial terraces have been identified: a 180-m (Inya) terrace and a 70-m (Saljar) terrace. We investigated the Inya terrace by excavating three pits along a profile; these pits cut through the loessic cover of the terrace to the underlying gravel. The surface of the terrace is uneven; closer to the valley side, there is a depression in the surface (Fig. 2), likely a relic of surface flow on the terrace as the flood waned. Pit location was selected to sample the different geomorphological settings of the terrace surface: (i) 18514 - in the depression close to the valley wall (2.1 m deep); (ii) 18515 - on the small terrace-like surface on the edge of the depression (1.1 m deep) and (iii) 18516 - on the terrace like surface at valley slope (1.6 m deep). The loess cover reached ~1m thick in the depression.

Sampling for luminescence dating was performed in the covered pits with no daylight exposure. A total of 24 samples for luminescence dating were collected from the three pits.

3. Sample preparation, analytical facilities and measurement protocols

Sample preparation took place in Moscow under dim orange light (Sohbati et al., 2017). Samples were processed using standard procedures (Murray et al., 2021): wet sieving to obtain the 180–250 µm sand fraction, followed by treatment with 10% HCl, H₂O₂, HF, and HCl. Density separation (2.58 g cm⁻³ aqueous heavy liquid solution of LST FastFloat™) was used provide quartz-rich and K feldspar-rich fractions. Finally the heavier quartz fraction was treated with 40% HF and 10% HCl to remove feldspar contamination and to etch the surface of the quartz grains. Clean quartz and K-rich feldspar grains were measured in Denmark. All measurements were made on multi-grain aliquots mounted on stainless steel discs (quartz, ~8 mm diam.; feldspar ~2 mm diam.) and measured in a Risø TL/OSL model DA-20 reader equipped with a calibrated beta source (Hansen et al., 2015). OSL was stimulated used blue light (470 ± 20 nm), and IRSL using infrared (870 ± 40 nm). The quartz OSL signal was detected through 7 mm of U-340 filter and K-rich feldspar Infrared Stimulated Luminescence (IRSL) through 4 mm of Corning 7–59 and 2 mm Schott BG 39 (Thomsen et al., 2008).

Quartz purity checks used the IR OSL depletion-ratio test (Duller, 2003); the average OSL IR depletion ratio is 0.988 ± 0.004 (n = 48; 24 samples) confirming the purity of the OSL signal from quartz extracts. Quartz dose estimates were made following a standard SAR protocol using a 260 °C preheat for 10 s, a 220 °C cut heat and an elevated temperature (280 °C) blue-light stimulation at the end of each SAR cycle (Murray and Wintle, 2000, 2003). The quartz OSL signal was measured with the sample held at 125 °C using blue light stimulation for 40s and

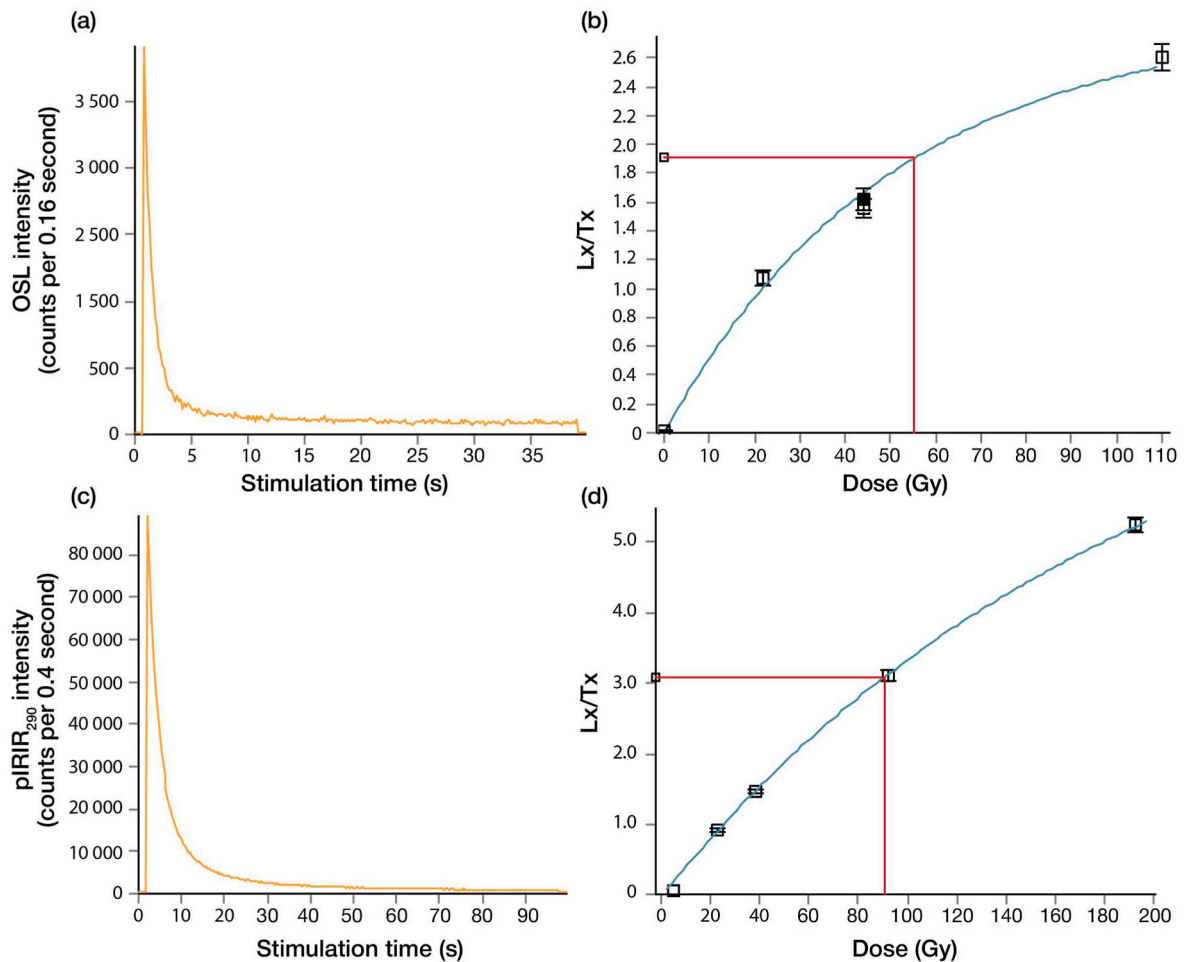


Fig. 3. Luminescence characteristics of quartz and K-rich feldspars grains.

early background subtraction (signal from first 0.32s minus that from subsequent 0.32s) was used to derive a net signal for further calculations. K-feldspar dose estimates were measured using a post-IR IRSL SAR protocol (Thiel et al., 2011; Buylaert et al., 2012) with thermal pre-treatments of 320 °C for 60 s after both regeneration doses and test doses, and an IR stimulation at 50 °C (for 200s) followed by an IR stimulation at 290 °C (for 200s) (pIRIR_{50,290}). Late background subtraction was used for net signal calculation using the signal from the initial 2 s minus that from the last 50 s of the decay curve. No correction was made for signal instability (Buylaert et al., 2012).

Radionuclide concentrations were measured using high resolution gamma spectrometry and the calibration method is described in Murray et al. (1987, 2018). Samples were dried, ground, ignited at 450 °C for 24 h, and mixed with high viscosity wax before casting in a cup shaped mould. The resulting ²³⁸U, ²²⁶Ra, ²³²Th and ⁴K activity concentrations were converted to dry infinite-matrix dose rates following Guérin et al. (2012). Water content corrections were as described by Aitken (1985) and cosmic ray contributions derived from Prescott and Hutton (1994).

4. Results

4.1. Loess cover structure

The structure of the sediments at the surface of the Inya terrace correlate with their geomorphological position (Fig. 2). Section descriptions are summarized in Table 1.

In all three pits, layers 1 is loess-like silts. In pits 18514 and 18515, layer 2 is formed from a mixture of loess-like silt and fine sand; this is

taken to be a transitional layer from loess to underlying colluvial layers, formed mainly from the characteristic sediment of the Inya catafluvial terrace. The bottom half of the deepest pit 18514 reflects reworked sediments of the catafluvial formation, reflecting different stages of slope process activity.

4.2. Luminescence chronology

4.2.1. Dose rate and water content

Radionuclide activity concentrations are summarized in Table 2, together with the assumed lifetime averaged water content. Water content assumptions are based on the current arid climate conditions and coarse material of the terraces which allows rapid draining of surface water. Total dose rate values generally correlate with the type of sediments and grain size: the smallest quartz dose rates are recorded in sands, $1.63 \pm 0.07 \text{ Gy ka}^{-1}$ (208883), and the largest in loess, between 3.13 ± 0.13 (208871) and $3.73 \pm 0.16 \text{ Gy ka}^{-1}$ (208888).

4.2.2. Quartz OSL and K-feldspar pIRIR ages

The quartz OSL signal of sand-sized grains from all samples is sensitive (e.g. Fig. 3a), and from a comparison with Risø calibration quartz (Hansen et al., 2015) it is dominated by the fast component. Fig. 3b presents a typical dose response curve (sample 208888) showing the accuracy of the sensitivity correction: recycling and OSL IR depletion ratio for this aliquot are indistinguishable from first regeneration dose point (open square at 45 Gy). Quartz dose recovery was measured for all samples in three pits: grains were bleached twice for 100s with blue light (with 10 ks pause in between) before giving a beta dose close to natural.

Table 3
Quartz and feldspar dose rate, dose, age and probable reliability.

Sample code	Depth (cm) ^a	FK IR ₅₀ ^b		FK pIRIR _{50,290} ^b		Q OSL ^b		WC %	Dr ^c	Age. ka			PWB ^d	WB ^d
		Dose, Gy	n	Dose, Gy	n	Dose, Gy	n			Gy/ka	Fk IR	Fk pIRIR _{50,290}		
208871	20	29 ± 2	6	53 ± 5	6	38.5 ± 3.3	20	10	3.13 ± 0.13	7.0 ± 0.6	13.0 ± 1.3	12.3 ± 1.2	✓	✓
208872	50	46 ± 4	6	75 ± 3	6	48.2 ± 4.2	16	10	2.75 ± 0.12	12.4 ± 1.1	20.5 ± 1.2	17.5 ± 1.7	✓	✓
208873	80	66 ± 6	6	106 ± 5	6	53.7 ± 5.8	21	10	2.84 ± 0.12	17.6 ± 1.8	28.0 ± 1.9	18.9 ± 2.2	✓	(✓)
208874	95	111 ± 6	6	173 ± 8	6	72.1 ± 10.4	21	10	2.99 ± 0.13	28.4 ± 1.8	44.0 ± 2.7	24.1 ± 3.7	✓	(✓)
208875	150	>400	6	>1000	6	112.0 ± 13.3	20	10	2.61 ± 0.11	>153.1	>281.8	42.9 ± 5.5		
208876	200	>400	6	>1000	6	>220.0	6	10	1.73 ± 0.07	>231.1	>374.8	>127.1		
208877	180	188 ± 13	6	284 ± 12	5	166.1 ± 6.7	16	10	1.99 ± 0.08	64.3 ± 5.0	97.1 ± 5.8	83.6 ± 5.1	✓	
208878	160	194 ± 9	6	366 ± 19	6	139.1 ± 8.0	18	10	2.03 ± 0.09	65.1 ± 3.8	123.3 ± 8.2	68.4 ± 5.1	✓	
208879	130	180 ± 10	6	278 ± 12	6	129.2 ± 4.8	20	10	1.95 ± 0.08	62.3 ± 4.1	96.3 ± 5.6	66.3 ± 3.9	✓	
208880	100	105 ± 8	6	173 ± 14	6	32.3 ± 1.5	18	10	2.03 ± 0.08	35.4 ± 2.8	58.5 ± 5.3	15.9 ± 1.0	(✓)	
208881	55	29 ± 2	6	60 ± 3	6	36.9 ± 2.5	18	10	2.50 ± 0.10	8.4 ± 0.5	17.5 ± 1.1	14.8 ± 1.2	✓	✓
208882	30	25 ± 2	6	46 ± 4	6	24.5 ± 1.6	22	10	2.44 ± 0.10	7.4 ± 0.6	13.8 ± 1.2	10.0 ± 0.8	✓	✓
208883	105	155 ± 6	8	244 ± 11	8	140.6 ± 17.3	2	10	1.63 ± 0.07	60.3 ± 3.1	95.3 ± 5.9	86.3 ± 11.3	✓	✓
208884	95	24 ± 1	8	49 ± 2	8	37.2 ± 2.0	20	10	2.53 ± 0.10	6.8 ± 0.5	14.0 ± 0.8	14.7 ± 1.0	✓	✓
208885	80	29 ± 2	8	62 ± 6	8	35.0 ± 1.0	19	10	2.63 ± 0.11	8.2 ± 0.6	17.4 ± 1.8	13.3 ± 0.7	✓	✓
208886	65	27 ± 2	2	54 ± 2	8	29.0 ± 2.0	19	10	2.92 ± 0.12	6.9 ± 0.5	14.0 ± 0.9	9.9 ± 0.8	✓	✓
208887	45	31 ± 0	2	58 ± 1	8	37.4 ± 1.8	19	10	3.57 ± 0.15	6.9 ± 0.3	12.9 ± 0.6	10.5 ± 0.7	✓	✓
208888	20	21 ± 6	2	49 ± 6	8	16.6 ± 1.3	12	10	3.73 ± 0.16	4.6 ± 1.2	10.5 ± 1.3	4.5 ± 0.4	✓	

^a Light gray - pit 18516; white - pit 18514; dark gray - pit 18515.

^b FK - K-rich feldspar, Q - quartz.

^c Total quartz dose rate, including cosmic ray contribution (Prescott and Hutton 1994), effect of water content (Aitken 1985) and assumed internal dose rate of 0.02 ± 0.01 Gy ka⁻¹. Feldspar dose rate can be derived by adding 0.94 Gy/ka (see text).

^d PWB - probably well bleached; WB - well bleached (see text).

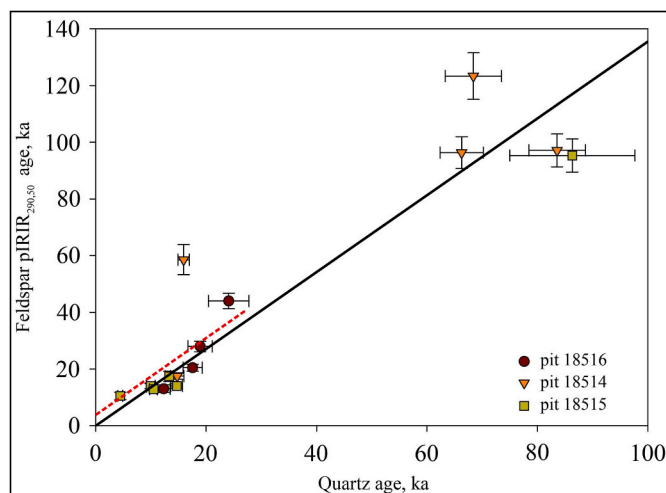


Fig. 4. Comparison of K-feldspar pIRIR_{50,290} and quartz OSL ages from different pits.

The average dose recovery ratio is 0.96 ± 0.01 ($n = 72$), indicating that our chosen SAR protocol is able to accurately measure a known laboratory dose given before any thermal pretreatment. Because we use multi-grain 8 mm aliquots, the measured OSL signals are summed over many grains. It is thus very unlikely that any incomplete bleaching will contribute to the distribution of doses. Because of this, and following the arguments of Guérin et al. (2015, 2017) and Murray et al. (2021), we take the arithmetic average of the quartz D_e estimates obtained using our selected protocol. These average D_e are summarized in Table 3, together with the standard deviations on the means (standard errors) and the number aliquots used to calculate the mean. Aliquots were rejected if they did not intersect the dose response curve (natural in saturation) or using the interquartile range (IQR) criterion (Medialdea et al., 2014). The quartz ages are also presented on Fig. 2.

Fig. 3c shows a typical pIRIR_{50,290} stimulation curve, and dose response curve. A dose recovery test was performed to test the suitability of our pIRIR_{50,290} protocol (six aliquots per sample). The natural signal was first reset in a Hönl daylight simulator for 48 h and different laboratory doses close to natural were then added. Test doses were ~50% of the given dose (Yi et al., 2016). For each sample, 3 aliquots were used to determine any residual dose, and 3 aliquots were given the known dose. After residual subtraction, the average pIRIR_{50,290} dose recovery ratio was 1.08 ± 0.03 ($n = 24$), indicating that our chosen protocol is able to accurately measure a known laboratory dose given before any thermal

pretreatment. For the reasons discussed above, individual D_e estimates are averaged arithmetically; the average doses and ages based on both IR₅₀ and pIRIR_{50,290} signals are summarized in Table 3, and the ages are also shown on Fig. 2.

The quartz OSL ages and K-feldspar pIRIR_{50,290} ages are more consistent for young samples and become less obviously close after 15–18 ka (Fig. 4, solid line of slope unity, no intercept). Closer examination suggests the presence of a small offset in the pIRIR_{50,290} young ages; this is indicated by the dashed line in Fig. 4 (fitted to the youngest ages with unit slope but unconstrained intercept). The intercept of this line is 3.5 ± 3.0 ka. In general, it is known that, of the three signals considered here, quartz OSL bleaches most quickly, followed by IR₅₀, followed by pIRIR_{50,290} (e.g. Murray et al., 2012). Table 3 compares the quartz ages with the IR₅₀ and pIRIR_{50,290} ages in the final two columns. Following Möller and Murray (2015), where the IR₅₀ ages are consistent with, or less than, the quartz ages, the latter are considered probably well bleached. Where the pIRIR_{50,290} ages are consistent with the OSL ages (after taking into account the offset of Fig. 4) then the quartz ages are considered well bleached. These identifications are probably conservative, as indicated by the quartz age of sample 208880, of 15.9 ± 1.0 ka. This is indistinguishable from the overlying age of sample 208881 of 14.8 ± 1.2 ka (identified as well bleached), and so the quartz signal of sample 208880 must also have been well bleached at deposition. Despite this, the IR₅₀ age is substantially older than the quartz age.

A similar argument can be made for the well bleached status of samples 208873 and 208874. In both cases the overlying sample is well bleached; since the underlying sample is indistinguishable in age, it must also be well bleached.

5. Discussion and conclusion

24 OSL ages were obtained from three pits on the surface of the Inya terrace. The deepest pit 18514 in the rear trough of the terrace showed the maximum loess thickness (~1 m). In this pit, quartz gives ages of 10–14 ka for loess layers 1 and 2, with all samples identified as well bleached. The sample from the bottom of the layer 3 has a quartz age of 15.9 ± 1.0 ka, and is identified as probably well bleached. Thus loess deposition in the depression on the terrace began around 16 ka. Layer 5 in this pit is interpreted as reflecting both different stages of reworking of the surface sediments, and colluvial transport from the elevated parts of the terrace and local valley slopes into the depression. All ages are identified as probably well bleached, and suggest two reworking events: at about 66–68 ka and 84 ka. The lowermost sample from layer 6 with classical catafluvial sediments has both quartz and feldspar in saturation. Thus we conclude that the oldest sediments in the depression on top of the catafluvial material are at least 84 ± 5 ka old.

The 18515 pit is located at a local terrace-like surface and elevated 4 m above the bottom of the depression. All samples are identified in Table 3 as probably well bleached, and all except the youngest as well bleached. The prolonged hiatus between L3 (bottom age 14.7 ± 1.0 ka) and L4 (86 ± 11 ka) suggests that part of the sequence has eroded. This is not surprising, as this site is at the highest elevation on the transect, and presumably at least some of the missing sediments were transported to the bottom of the depression at the east side of the terrace surface. These erosional events occurred after 86 ka, and exposed the old surface of the terrace to post-LGM loess deposition.

In the 18516 pit, all samples are identified in Table 3 as well bleached, except for the oldest (layer 3, 43 ± 6 ka) for which no conclusion can be drawn. Layer 1 gives a younger age of 12.3 ± 1.2 ka, and layer 2 form during and after the LGM. The single sample of Layer 3 is of unknown status, but clearly not inconsistent with older ages identified as reliable from the other two pits.

Correlation of the loess layers of three pits clearly indicates that the surface of the Inya terrace was available to loess accumulation at around 14–16 ka, i.e. post-LGM. Between the loess cover and the catafluvial gravel deposits there is a well-defined layer of reworked sands, from

which a set of ages describing three stages of the terrace surface reworking before the LGM. Sand layers in the depth interval of 0.7–1.0 (18516) m gave ages in the range of 18–25 ka, which correlated with the ¹⁰Be dates obtained from boulders on the surface of the neighboring Yaloman bar (left side of the Katun valley) - ~18 ka. (Reuther et al., 2006, recalculated by Gribenski et al., 2016). In addition, the series of older ages from pits 18515 and 18514 record two reworking events at 66–68 and 83–86 ka.

From these results, we conclude that the Inya bar was formed no later than 83–86 ka ago. This age is in good agreement with the only IRSL age from the alluvial terrace adjacent to a similar bar in the mouth of the Maly Yaloman river (89 ± 10 ka) (Deev et al., 2019). The loess cover that formed on the bar surface up to the LGM is missing, and was probably periodically destroyed. The last cycle of accumulation of cover sediments dates to late MIS 2. In the first half of MIS 2, any previously accumulated loess was presumably washed into the depression which now acts as a sediment trap. Thus our results provide evidence in favour of bar formation during MIS 5 and the development of a post-LGM geomorphological surface of the catafluvial Inya bar of Altai Mountains.

Declaration of competing interest

The authors declare that they have no known competing financial interests or personal relationships that could have appeared to influence the work reported in this paper.

Acknowledgments

Svistunov, Kurbanov, Taratunina, Semikolenykh, Entin, Deev, Zolnikov, and Panin have removed their academic affiliations because sanctions following the Ukraine-Russian conflict prevent Danish researchers (Murray) publishing with Russian state institutions. This research was supported by project 19-17-00179 “Glacial history and catastrophic processes in Russia Altai in the Late Pleistocene – Holocene” (field work and luminescence dating), N. Taratunina was supported by program N^o 121051100135-0 (sample treatment) and A.V. Panin acknowledges the support of program N^o FMGE-2019-0004.

References

- Aitken, M.J., 1985. Thermoluminescence Dating. Academic Press, London.
- Baker, V.R., 2013. Global late quaternary fluvial palaeohydrology: with special emphasis on palaeofloods and megafloods. *Treat. Geomorphol.* 511–527.
- Baker, V., Benito, G., Rudoy, A., 1993. Palaeohydrology of late Pleistocene superflooding, altay Mountains, siberia. *Science* 259, 348–350.
- Bohorquez, P., Jimenez-Ruiz, P.J., Carling, P.A., 2019. Revisiting the dynamics of catastrophic late Pleistocene glacial-lake drainage, Altai Mountains, central Asia. *Earth Sci. Rev.* 197, 102892.
- Butvilovskij, V.V., 1993. Palaeogeography of the Last Glaciation and Holocene Altai Event-Catastrophic Model. *Izdatelstvo Tom. un-ta, Tomsk (In Russian)*.
- Buylaert, J.-P., Jain, M., Murray, A.S., Thomsen, K.J., Thiel, C., Sobhati, R., 2012. A robust feldspar luminescence dating method for Middle and Late Pleistocene sediments. *Boreas* 41, 435–451.
- Buylaert, J.-P., Yeo, E.Y., Thiel, C., Yi, S., Stevens, T., Thompson, W., Frechen, M., Murray, A.S., Lu, H., 2015. A detailed post-IR IRSL chronology for the last interglacial soil at the Jingbian site (northern China). *Quat. Geochronol.* 30, 194–199.
- Carling, P.A., 2013. Freshwater megaflood sedimentation: what can we learn about generic processes? *Earth Sci. Rev.* 125, 87–113.
- Carling, P.A., Kirkbride, A.D., Parnachov, S., Borodavko, P.S., Berger, G.W., 2002. Late Quaternary catastrophic flooding in the Altai Mountains of south-central Siberia: a synoptic overview and an introduction to flood deposit sedimentology. In: Martini, I. P., Baker, V.R., Garzón, G. (Eds.), *Flood and Megaflood Processes and Deposits*.
- Carling, P.A., Villanueva, I., Herget, J., Wright, N., Borodavko, P., Morvan, H., 2010. Unsteady 1D and 2D hydraulic models with ice dam break for Quaternary megaflood, Altai Mountains, southern Siberia. *Global Planet. Change* 70 (1–4), 24–34.
- Carling, P.A., Bristow, C.S., Litvinov, A.S., 2016. Ground-penetrating radar stratigraphy and dynamics of megaflood gravel dunes. *J. Geol. Soc.* 173 (3), 550–559.
- Deev, E., Turova, I., Borodovskiy, A., Zolnikov, I., Pozdnyakova, N., Molodkov, A., 2019. Large earthquakes in the Katun fault zone (Gorny Altai): palaeoseismological and archaeoseismological evidence. *Quat. Sci. Rev.* 203, 68–89.
- Duller, G.A.T., 2003. Distinguishing quartz and feldspar in single grain luminescence measurements. *Radiat. Meas.* 37, 161–165.

- Gribenski, N., Jansson, K.N., Lukas, S., Stroeven, A.P., Harbor, J.M., Blomdin, R., Ivanov, M.N., Heyman, J., Petrakov, D.A., Rudoy, A., Clifton, T., Lifton, N.A., Caffee, M.W., 2016. Complex patterns of glacier advances during the late glacial in the chagan Uzun valley, Russian Altai. *Quat. Sci. Rev.* 149, 288–305.
- Guérin, G., Mercier, N., Nathan, R., Adamiec, G., Lefrais, Y., 2012. On the use of the infinite matrix assumption and associated concepts: a critical review. *Radiat. Meas.* 47, 778–785.
- Guérin, G., Jain, M., Thomsen, K.J., Murray, A.S., Mercier, N., 2015. Modelling dose rate to single grains of quartz in well-sorted sand samples: the dispersion arising from the presence of potassium feldspars and implications for single grain OSL dating. *Quat. Geochronol.* 27, 52–65.
- Guérin, G., Christophe, C., Philippe, A., Murray, A.S., Thomsen, K.J., Tribolo, C., Urbanova, P., Jain, M., Guibert, P., Mercier, N., Kreutzer, S., Lahaye, C., 2017. Absorbed dose, equivalent dose, measured dose rates, and implications for OSL age estimates: introducing the Average Dose Model. *Quat. Geochronol.* 41, 163–173.
- Hansen, V., Murray, A., Buylaert, J.P., Yeo, E.Y., Thomsen, K., 2015. A new irradiated quartz for beta source calibration. *Radiat. Meas.* 81, 123–127.
- Herget, J., 2005. Reconstruction of Pleistocene Ice-Dammed Lake Outburst Floods in Altai-Mountains, vol. 386. Geological Society of America, Special Publication. <https://doi.org/10.1130/0-8137-2386-8.1>.
- Huang, W., Cao, Z.-X., Carling, P.A., Pender, G., 2014. Coupled 2D hydrodynamic and sediment transport modeling of megaflood due to glacier dam-break in Altai Mountains, Southern Siberia. *J. Mt. Sci.* 11 (6), 1442–1453.
- Krivonogov, S., Zolnikov, I., Novikov, I., Deev, E., 2017. Giant glaciogenic floods in the Altai – geomorphological. In: Geological and Hydrological Aspects – Guidebook for Field Excursion at the 14th International Workshop on Present Earth Surface Processes and Longterm Environmental Changes in East Eurasia, Novosibirsk, September 15–21, 2017, pp. 17–29.
- Lehmkuhl, F., Zander, A., Frechen, M., 2006. Luminescence chronology of fluvial and aeolian deposits in the Russian Altai (Southern Siberia). *Quat. Geochronol.* 2, 195–201.
- Medialdea, A., Thomsen, K.J., Murray, A.S., Benito, G., 2014. Reliability of equivalent-dose determination and age-models in the OSL dating of historical and modern palaeoflood sediments. *Quat. Geochronol.* 22, 11–24.
- Möller, P., Murray, A., 2015. Drumlinised glaciofluvial and glaciolacustrine sediments on the Småland peneplain, South Sweden – new information on the growth and decay history of the Fennoscandian Ice Sheets during MIS 3. *Quat. Sci. Rev.* 122 <https://doi.org/10.1016/j.quascirev.2015.04.025>.
- Murray, A.S., Wintle, A.G., 2000. Luminescence dating of quartz using an improved single-aliquot regenerative-dose protocol. *Radiat. Meas.* 32 (1), 57–73.
- Murray, A.S., Wintle, A.G., 2003. The single aliquot regenerative dose protocol: potential for improvements in reliability. *Radiat. Meas.* 37, 377–381.
- Murray, A.S., Marten, R., Johnston, A., Martin, P., 1987. Analysis for naturally occurring radionuclides at environmental concentrations by gamma spectrometry. *J. Radioanal. Nucl. Chem.* 115, 263–288.
- Murray, A.S., Thomsen, K.J., Masuda, N., Buylaert, J.-P., Jain, M., 2012. Identifying well-bleached quartz using the different bleaching rates of quartz and feldspar luminescence signals. *Radiat. Meas.* 47 (9), 688–695. <https://doi.org/10.1016/j.radmeas.2012.05.006>.
- Murray, A.S., Helsted, L.M., Autzen, M., Jain, M., Buylaert, J.-P., 2018. Measurement of natural radioactivity: calibration and performance of a high-resolution gamma spectrometry facility. *Radiat. Meas.* 120, 215–220.
- Murray, A., Lee, J.A., Buylaert, J.-P., Guérin, G., Qin, J., Singhvi, A.K., Smedley, R., Thomsen, K.J., 2021. Optically stimulated luminescence dating using quartz. *Nat. Rev. Meth. Primers* 1, 72.
- Panin, A., Baryshnikov, G., 2015a. Old valley of Chuya - its age and mechanism of abandonment. In: Baryshnikov, G., Agatova, A., Carling, P., Herget, J., Panin, A., Adamiec, G., Nepop, R. (Eds.), *Russian Altai in the Last Pleistocene and the Holocene – Geomorphological Catastrophes and Landscape Rebound (Fieldtrip Guide)*. Barnaul, ASU Publ., pp. 115–119.
- Panin, A., Baryshnikov, G., 2015b. The Chuya spillway upstream from Chibit town. In: Baryshnikov, G., Agatova, A., Carling, P., Herget, J., Panin, A., Adamiec, G., Nepop, R. (Eds.), *Russian Altai in the Last Pleistocene and the Holocene – Geomorphological Catastrophes and Landscape Rebound (Fieldtrip Guide)*. Barnaul, ASU Publ., pp. 112–114.
- Parnachev, S.V., 1999. Geology of High Altai Terraces (Yalmano-Katunskaya Zona). IPF TPU, Tomsk.
- Prescott, J.R., Hutton, J.T., 1994. Cosmic ray contributions to dose rates for luminescence and ESR dating: large depths and long-term time variations. *Radiat. Meas.* 23, 497–500.
- Reuther, A.U., Herget, J., Ivy-Ochs, S., Borodavko, P., Kubik, P.W., Heine, K., 2006. Constraining the timing of the most recent cataclysmic flood event from ice-dammed lakes in the Russian Altai Mountains, Siberia, using cosmogenic in situ ¹⁰Be. *Geology* 34 (11), 913–916. <https://doi.org/10.1130/G22755A.1>.
- Rudoy, A.N., 1995. Geomorphological effect and hydraulics of the Late Pleistocene jokullaups of glacial dammed lakes in southern Siberia. *Geomorfologija* 4, 61–76 (In Russian).
- Rudoy, A.N., 2001. Hydraulic characteristics and possible geochronology of Quaternary glacial superfloods in Altai. *Izvestija RGO* 133 (5), 30–41 (In Russian).
- Rudoy, A., 2002. Glacier-dammed lakes and geological work of glacial superfloods in the late Pleistocene, southern Siberia, Altai Mountains. *Quat. Int.* 87, 119–140.
- Rudoy, A., 2005. Giant Current Ripples - History of the Research, Their Diagnostics and Palaeogeographical Significance. Tomsk.
- Rudoy, A.N., Baker, V.R., 1993. Sedimentary effects of cataclysmic late Pleistocene glacial outburst flooding, Altai Mountains, Siberia. *Sediment. Geol.* 85, 53–62.
- Sohbati, R., Murray, A., Lindvold, L.R., Buylaert, J.-P., Jain, M., 2017. Optimization of laboratory illumination in optical dating. *Quat. Geochronol.* 39, 105–111.
- Thiel, C., Buylaert, J.-P., Murray, A.S., Terhorst, B., Hofer, I., Tsukamoto, S., Frechen, M., 2011. Luminescence dating of the Stratzing loess profile (Austria) - testing the potential of an elevated temperature post-IR IRSL protocol. *Quat. Int.* 234, 23–31.
- Thomsen, K.J., Murray, A.S., Jain, M., Bøtter-Jensen, L., 2008. Laboratory fading rates of various luminescence signals from feldspar-rich sediment extracts. *Radiat. Meas.* 43, 1474–1486.
- Yi, S., Buylaert, J.-P., Murray, A.S., Lu, H., Thiel, C., Zeng, L., 2016. A detailed post-IR IRSL dating study of the Niuyangzigou loess site in northeastern China. *Boreas* 45, 644–657.
- Zolnikov, I.D., Deev, E.V., Kurbanov, R.N., Panin, A.V., Vasil'ev, A.V., Pozdnjakova, N.I., Turova, I.V., 2021. The age of the chibit glaciation of Gorny Altai. *Doklady Rossijskoj Akademii Nauk. Nauki o Zemle* 496 (2), 204–210 (In Russian).
- Zolnikov, I.D., Deev, E.V., Rusanov, G.G., Nazarov, D.V., Kotler, S.A., 2016. New results of OSL-dating of Quaternary sediments of the upper Katun valley (Gorny Altai) and adjacent territory. *Geologija i geofizika* 57 (6), 1194–1197 (In Russian).